Host-guest complexes of C-propyl-2-bromoresorcinarene with aromatic *N*-oxides

Rakesh Puttreddy,[a] Ngong Kodiah Beyeh,[b,c] Pia Jurček,[a] Lotta Turunen,[a] John F. Trant,[c] Robin H. A. Ras[b] and Kari Rissanen[a]*

[a]*University of Jyvaskyla, Department of Chemistry, Nanoscience Center, P. O. Box 35, FI-40014 University of Jyvaskyla, Finland.*

[b]*Aalto University, School of Science, Department of Applied Physics, Puumiehenkuja 2, 02150 Espoo, Finland.*

[c]*University of Windsor, Department of Chemistry and Biochemistry, Windsor, ON, N9B 3P4 Canada.*

*Corresponding author. Email: *kari.t.rissanen@jyu.fi*

Dedicated to Professor Jerry L. Atwood on the occasion of his 75th Anniversary

Host-guest complexes of *C*-propyl-2-bromoresorcinarene with aromatic *N*-oxides

Abstract: The host-guest complexes of *C*-propyl-2-bromoresorcinarene with pyridine *N*-oxide, 3-methylpyridine *N*-oxide, quinoline *N*-oxide and isoquinoline *N*-oxide are studied using single crystal X-ray crystallography and ^{1}H NMR spectroscopy. The *C*-propyl-2-bromoresorcinarene forms *endo*-complexes with the aromatic *N*-oxides in the solid-state when crystallised from either methanol or acetone. In solution, the *endo*-complexes were observed only in methanol-d_4. In DMSO the solvent itself is a good guest, and crystallization provides only solvate *endo*-complexes. The *C*-propyl-2-bromoresorcinarene shows remarkable flexibility when crystallised from either methanol or acetone, and packs into one-dimensional self-included chains. Of special note, crystallizing *C*-propyl-2-bromoresorcinarene with 3-methylpyridine *N*-oxide from acetone results in a 2:2 dimeric capsular assembly organized through both C−H···π_{host} and N−O···(H−O)$_{host}$ interactions.

Keywords: Supramolecular Chemistry; Resorcinarenes; Aromatic *N*-oxides; Hydrogen bonds; Crystal structure

Dedicated to Professor Jerry L. Atwood on the occasion of his 75th Anniversary

1. Introduction

Resorcinarenes are aromatic macrocyclic compounds widely used in supramolecular chemistry as prototypical building blocks for the design of hierarchical architectures (*1*). These receptors are widely used in host-guest chemistry for various molecular recognition processes (*1*). Their accessibility from inexpensive starting materials and their easy synthetic modification makes resorcinarenes excellent scaffolds for obtaining a wide variety of structurally-defined derivatives. These have been used for catalysis, stabilizing unstable species, and recognizing and differentiating between various neutral and ionic guests (*2*). When in their C_{4v} conformation, the bowl-shaped confined cavity is mainly responsible for their guest-recognition properties with size-, solvent- and structure-dependent selectivity (*1a,1b*,*2*). The intra-, and to lesser extent, inter-molecular, O−H···O hydrogen bonds (HBs) determine the C_{4v} conformation; however, they can show remarkable conformational flexibility by responding to minute changes in their environment, such as temperature, solvent, or the nature of the guest molecules (*1-3*). This responsive but limited geometric flexibility, has played a key role in the design and construction of dimeric, tetrameric, hexameric or 1-D chain resorcinarene-derived supramolecular constructs *via* self-assembly processes (*4*). Resorcinarenes can self-assemble without any guests (*5*), as was demonstrated by the first solid-state hexameric capsule by Atwood and MacGillivray over 20 years ago (*6*). This iconic work has inspired several groups, including our own, to explore the guest-to-host transformations of the resorcinarene cavity size and shape both in solution and in the solid-state (*7*). Among the non-covalent host-guest interactions responsible for self-assembly processes, the *endo*-cavity C−H···π interactions play a particularly important role in the molecular recognition events both in solution and in the solid-state (*8*).

Heterocyclic guest molecules persist as important targets in supramolecular host-guest

chemistry, and resorcinarenes are good hosts for five- and six-membered aromatic *N*-heterocycles *(9)*. Co-crystals of many flexible and rigid heterocyclic aromatic guests have been extensively studied to understand the conformation, the nature of the *endo*-cavity complex formation, and the outcome of the $N\cdots(H{-}O)_{host}$ HB competition between the potential intra-host and solvent-host non-covalent interactions (*1*, *9*). Aromatic *N*-oxides are potent HB acceptors and can interact simultaneously with up to three different hydroxyl groups, a feature not available for their parent *N*-heterocyclic analogues. The zwitterionic $N^{+}{-}O^{-}$ and the multidentate acceptor capacity of the *N*-oxide for multiple strong $N{-}O\cdots(H{-}O)_{host/solvent}$ interactions makes *N*-oxides challenging targets for rationally designing specific resorcinarene *endo*-complexes. However, the electron push-pull nature of the N−O group renders them suitable guests for *endo*-complexation through π–π and C−H···π interactions between the electron-rich π-cavity of the host and the electron-deficient aromatic *N*-oxide guests (*10*). Recently, we have reported several studies on the host-guest complexation of various aromatic *N*-oxides with differentially substituted resorcinarenes (*11*). The nature of the upper rim substituents at the 2-position of the resorcinarene host (Figure 1) have a direct effect both on the conformation and electronic properties of the receptor. The size of the aromatic *N*-oxide guest, the nature of the substituents at the 2-position of the resorcinarene skeleton, and the length of the resorcinarene's lower rim alkyl chains, all play a role in determining the mode of complexation. For example, in the methyl-resorcinarene (**C1**) *N*-oxide complexes, the host mainly prefers to adopt a *boat*-conformation (C_{2v}), and readily organizes into 1-D tubular chains driven by *N*-oxide·N–$O\cdots(H{-}O)_{host}$ *exo*-interactions (*11a*). By introducing a methyl substituent to the 2-position and an ethyl chain to the lower rim (**MeC2**, Figure 1), the *N*-oxide *endo*-complexation process is remarkably improved, and instead of the 1-D chains, 1:1 host-

guest *endo*-complexes are observed (*11b-e*). Clearly, both the conformational flexibility of the host and the C-H acidity of the *ortho*-protons of the *N*-oxide guest play vital roles in defining the complexation. This is further illustrated by the **BrC2** *N*-oxide complexes (Figure 1), where the presence of the electron-withdrawing bromine enhances the O-H acidity and thus renders the host more rigid. This enables better encapsulation of small guest molecules (*11f*). In these more rigid *endo*-complexes, the position and orientation of the aromatic *N*-oxide guest allows for strong C–H···π_{host} interactions with the cavity walls. To gain deeper insight into the influence of the Br-atom at the 2-position on the supramolecular behaviour, we have expanded our study to the inclusion complexes of C-propyl-2-bromoresorcinarene (**BrC3**) with selected aromatic *N*-oxides in both solution and the solid-state. In this study, we have used pyridine *N*-oxide (**1**), 3-methylpyridine *N*-oxide (**2**), quinoline *N*-oxide (**3**) and isoquinoline *N*-oxide (**4**) as guest molecules to study the solvent effects on 1:1 host-guest *endo*-complexation processes (Figure 1). Although resorcinarene-based host-guest complexes have been extensively explored, and well characterized in the solid-state by single crystal X-ray analysis, no single crystal structures of **BrC3** have been deposited in the Cambridge Structural Database (12).

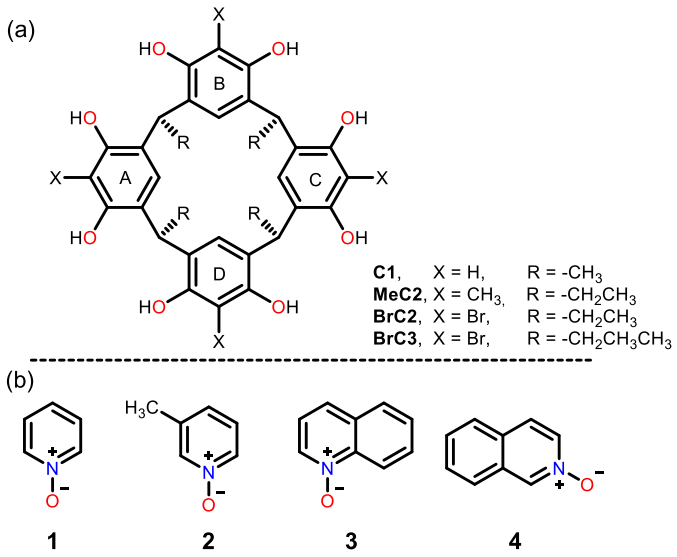

Figure 1. (a) Chemical structures of the core resorcinarenes, (aromatic rings labelled as A-D) and (b) guests investigated in the current study: pyridine *N*-oxide (**1**), 3-methylpyridine *N*-oxide (**2**), quinoline *N*-oxide (**3**) and isoquinoline *N*-oxide (**4**).

2. Experimental section

2.1. Materials and methods

All the solvents used for both synthesis and crystallizations were reagent grade, and were used as received. Pyridine *N*-oxide (**1**), 3-methylpyridine *N*-oxide (**2**), quinoline *N*-oxide (**3**) and isoquinoline *N*-oxide (**4**) were purchased from Sigma Aldrich while C-propyl-2-bromoresorcinarene (**BrC3**) was synthesized using reported procedures (*13*). The ^{1}H NMR spectra were recorded on a Bruker Avance DRX 500 MHz spectrometer and the deuterated solvents used for all ^{1}H NMR analysis were purchased from Sigma Aldrich. Single crystal X-ray data for all complexes were collected at either 120 or 170 K using a Rigaku-Oxford Supernova Diffractometer or a Bruker-Nonius Kappa CCD diffractometer (See supporting information for more details).

3. Results and Discussion

3.1. Solution studies

The host-guest complexations between the host, **BrC3** and *N*-oxide guests (**1**, **2**, **3** and **4**), were first studied in solution through a series of ^{1}H NMR experiments in three hydrogen bond competitive solvents: acetone, methanol (MeOH) and dimethylsulfoxide (DMSO). The ^{1}H NMR spectra of **BrC3** confirmed the preference for the C_{4v} symmetry as expected, as only one set of resonances is observed, indicating that the host adopts the crown conformation (Figure 2). In all of our previous solution-state studies carried out in MeOH-d_4 (*11*), the hydrogen bond interactions between host and guest were not

observed due to fast H/D exchange processes on the NMR time scale at 298 K. In MeOH-d_4, several independent complexation-induced chemical shift changes of the guest resonances were observed, presumably due to electronic shielding effects of the aromatic rings of the host cavity. For example (Figure 2a), significant up-field shift changes, up to 0.28 ppm, for the *d and e* protons along with smaller up-field shifts for the *ortho*-protons *a* and *g* (0.08 and 0.06 ppm respectively) of guest **4** are observed. This suggests that in solution, the N-O group of guest **4** is pointing outwards from the **BrC3** cavity during *endo*-complexation. The ^{1}H NMR experiments for guests **1**, **2** and **3** (Figure S1, S2 and S3) show similar up-field chemical shift changes for the aromatic rings suggesting *N*-oxides are encapsulated inside the cavity through C-H···π interactions with N-O group pointing outside of the cavity.

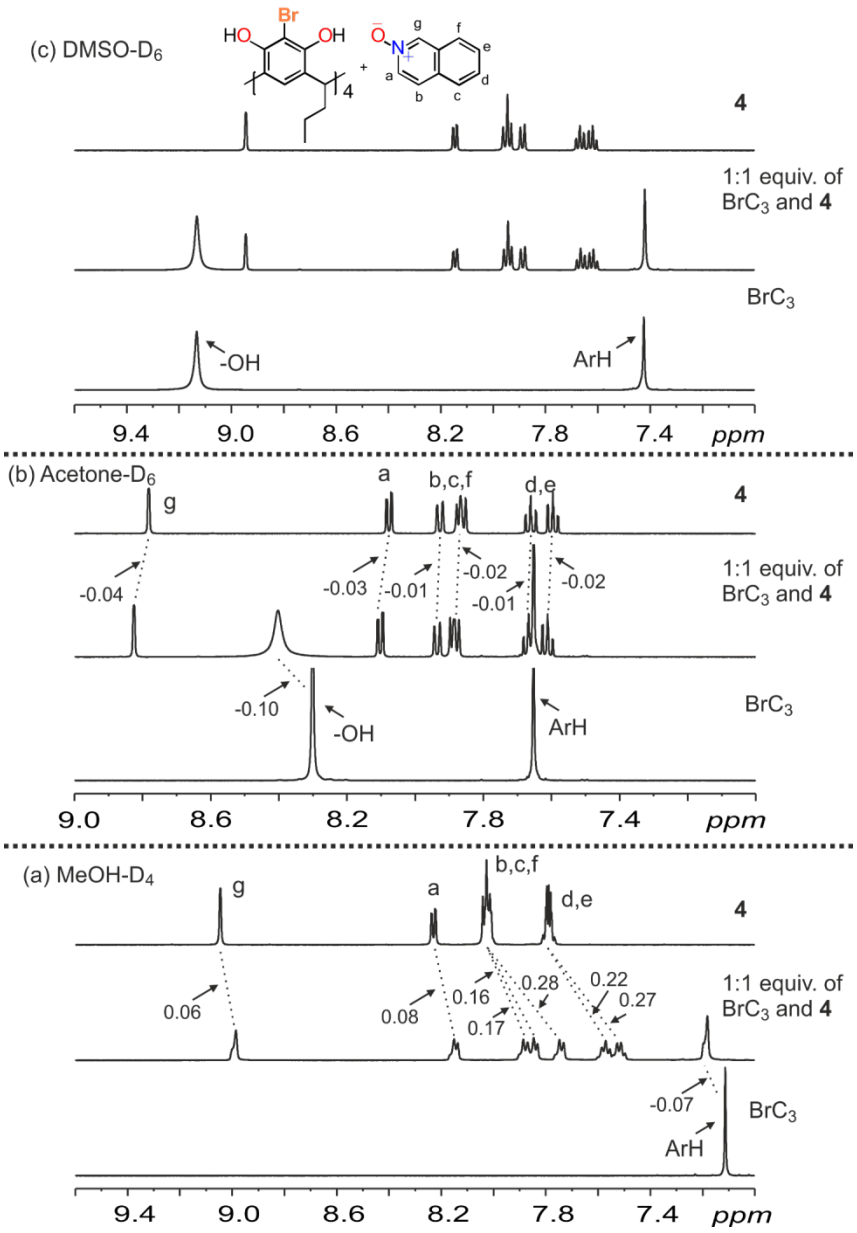

Figure 2. An expansion of the ^{1}H NMR (6.6 mM at 298 K, 500 MHz) of **BrC3** complexes with **4**. Spectra are produced from **BrC3**, **4** and an equimolar mixture of **BrC3** and **4** in: (a) MeOH-d_4, (b) acetone-d_6 and (c) DMSO-d_6. Dashed lines highlight the observed shift changes of the resonances, labels are in ppm.

In DMSO-d_6 and acetone-d_6, H/D exchange processes are not expected, thus any extant HB interactions should be observed. In DMSO-d_6, under similar experimental conditions to those used in MeOH-d_4, no chemical shift changes were observed from the NMR spectra of an equimolar mixture of **BrC3** and *N*-oxides, strongly suggesting that no *endo*-cavity host-guest interactions exist in solution (Figure 2c, S1-S2). The

DMSO would be expected to heavily solvate both the **BrC3** and the *N*-oxide guests, likely preventing the components from interacting. Under similar conditions in acetone-d_6, and again using a mixture of **BrC3** and **4** as an example, moderate deshielding of the hydroxyl groups of the **BrC3** receptor (-0.10 ppm) is observed which confirms hydrogen bonding between the host and the *N*-oxide guests. Interestingly, no shielding of the *N*-oxide guest resonances is observed. In fact, a small deshielding effect of the guest signals is observed (Figures 2b), which likely results from hydrogen bonding between the hydroxyl groups of the host and the O-atom of the *N*-oxide guest. This process results in a decrease in electron density on the *N*-oxide and is consistent with the observed deshielding effect. This phenomenon is also observed between the **BrC3** host and all the other aromatic *N*-oxide guests in acetone (Figure S1-S3). In bulk acetone-d_6, clearly the hydrogen bonding between the **BrC3** host and the *N*-oxide guests is the major interaction as the *N*-oxide is a better hydrogen bond acceptor than acetone. In addition, acetone prefers to reside inside the **BrC3** cavity. Consequently, in acetone solution, the solvent out-competes the *N*-oxides in occupying the cavity and forces the *N*-oxide guests to interact with the resorcinarenes as hydrogen-bonded *exo*-complexes; however, in protic solvents *i.e.*, MeOH, the *N*-oxides preferentially reside in the cavity, and this favours the formation of the observed *endo*-complexes.

3.2 Single crystal X-ray crystallography

Single crystals of all complexes were obtained from slow evaporation of the respective solutions of a 1:1 molar ratio of host and guest molecules, except for complexes **2**@**BrC3**_acetone-d_6 and **3**@**BrC3**_acetone-d_6, which were obtained by slow evaporation from a 1:1 molar mixture of the host and guest from an acetone-d_6 solution. Unlike crystals obtained from MeOH and acetone, the DMSO crystallization produces large block-like crystals consisting only of an *endo*-/*exo*-DMSO

solvate, DMSO@**BrC3**_DMSO, regardless of the *N*-oxide used. The crystal lattice contains no *N*-oxide guests. This is due to both the competitive nature of DMSO as a guest and also the very favourable solvation of the putative *N*-oxide guests by DMSO and their consequent preference to reside in solution. This phenomenon is well-supported by the ^{1}H NMR experiments described above.

The BrC3 crystallizations without the guest

Before examining the solid-state complexation with *N*-oxide guests, we crystallized the host resorcinarene from the different solvents to provide structural comparisons. Consequently, the **BrC3** host was crystallized from methanol [**BrC3**] and acetone [**BrC3**•acetone]. In both cases, it packs into self-included 1-D polymeric chains, as shown in Figure 3a and b. In the **BrC3** from methanol, the Br···Br distances between the adjacent hosts are longer than the sum of van der Waals radii, while in **BrC3**•acetone Br···Br distances are slightly shorter (3.51 Å, sum Br_{VDW} = 3.70 Å). In our previous study (*13*), when **BrC2** was crystallized from acetone, both the **BrC2** cavity and the space in between the alkyl chains were occupied by acetone molecules stabilized through *endo*-C–H···π and C=O···H–C interactions (Figure 3d). The resorcinarene cavity in **BrC3**•acetone, however, prefers to form a self-inclusion complex so that only the space in between the alkyl chains is occupied by acetone molecules (Figure 3b and e). In contrast to methanol and acetone that encourage the formation of self-included chain structures, the DMSO solvate forms an *endo*-complex, DMSO@**BrC3**. The asymmetric unit contains six DMSO molecules with a multitude of S=O···H–O and O···H–O HB interactions (Figure 3c). In DMSO@**BrC3**, one of the *exo*-DMSO sulphur atoms interacts with the resorcinarene bromine through a weak S···Br halogen bond (XB) of 3.41 Å (R_{XB} = 0.93) (*14*). Both **BrC3**•acetone and DMSO@**BrC3**

incorporate solvents in their lower rim through X=O···H−C (X = C and S) interactions, while the **BrC3** crystal obtained from methanol is solvent-free.

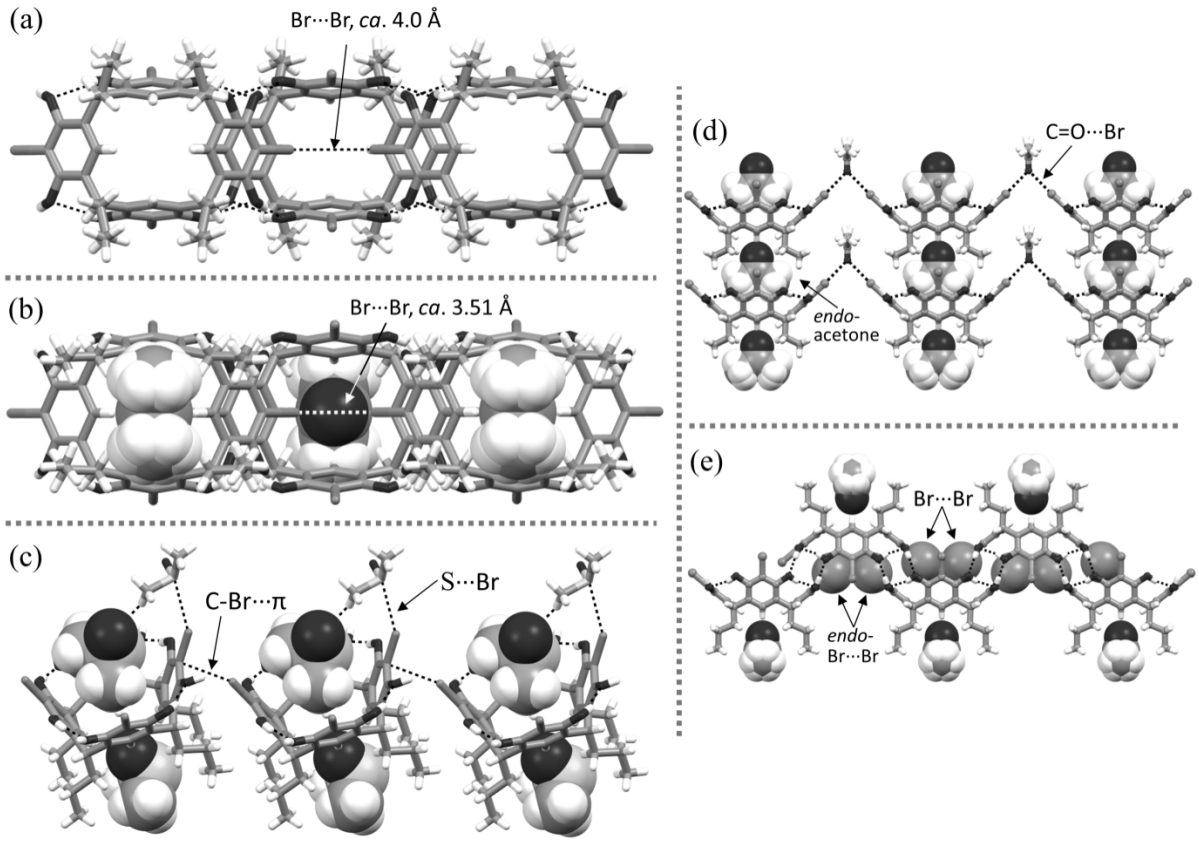

Figure 3. A segment of the 1-D polymeric self-included structures (a) **BrC3** from methanol and (b) **BrC3•**acetone shown to compare *endo*-Br···Br interactions. (c) The DMSO**@BrC3** displays S···Br and C−Br···π interactions**.** Comparison of our previously reported structure acetone**@BrC2** (d, *11f*) with **BrC3•**acetone (e). Selected solvent molecules and the self-included bromines in (e) are shown as CPK models.

The BrC3-*N*-oxide complexes from methanol

Complexes obtained from MeOH with pyridine *N*-oxide (**1**@**BrC3**_MeOH) and 3-methylpyridine *N*-oxide (**2**@**BrC3**_MeOH) form *endo*-complexes, while isoquinoline *N*-oxide (**4•BrC3**_MeOH) forms an *exo*-complex, in complete contrast to the results observed by ^{1}H NMR in solution. Unfortunately, with

quinoline *N*-oxide **3**, all attempts to obtain single crystals from MeOH were unsuccessful. In **1@BrC3**_MeOH, the *endo*-*N*-oxide $(O-H)_{host}\cdots(N-O)\cdots(H-O)_{MeOH}$ and C−Br···π (*ca*. 3.21 Å) interactions between adjacent host molecules leads to the formation of 1-D chains (Figure 4a). These 1-D chains are further extended into 2-D polymeric sheet-like structures through additional *exo*-*N*-oxides bridging the –OH groups of adjacent hosts. In **2@BrC3**_MeOH, both the *endo*-cavity and the space between the lower rim propane chains are occupied by aromatic *N*-oxides through C–H···π and N–O···H–C interactions respectively (See supporting information Figures S4 and S5 for *endo*-*N*-oxide C–H···π interactions), with the distances ranging between 2.61–2.89 Å and 2.48–2.71 Å, respectively. The *endo*-*N*-oxides assist the formation of 1-D chains through $(O-H)_{host}\cdots(N-O)\cdots(H-O)_{host}$ interactions, while the additional *exo*-*N*-oxides decorate the periphery of the 1-D chains *via* direct HBs to host -OH groups. In **4•BrC3**_MeOH, the **BrC3** host forms self-included 1-D chains, similar to those observed for **BrC3** crystallized from methanol or acetone described above. In this structure, the *N*-oxide guest resides outside the cavity, forming an *exo*-complex, and interacts with the host through HBs to the −OH groups. As shown in Figure 4c, the *exo*-*N*-oxide guest shows $C-Br\cdots\pi_{guest}$ interactions at distances of 3.27 Å. The 1-D chains propagate into 2-D sheet-like structures through several π-π interactions between adjacent hosts' aromatic rings and through bidentate $(O-H)_{host}\cdots(N-O)\cdots(H-O)_{host}$ HBs.

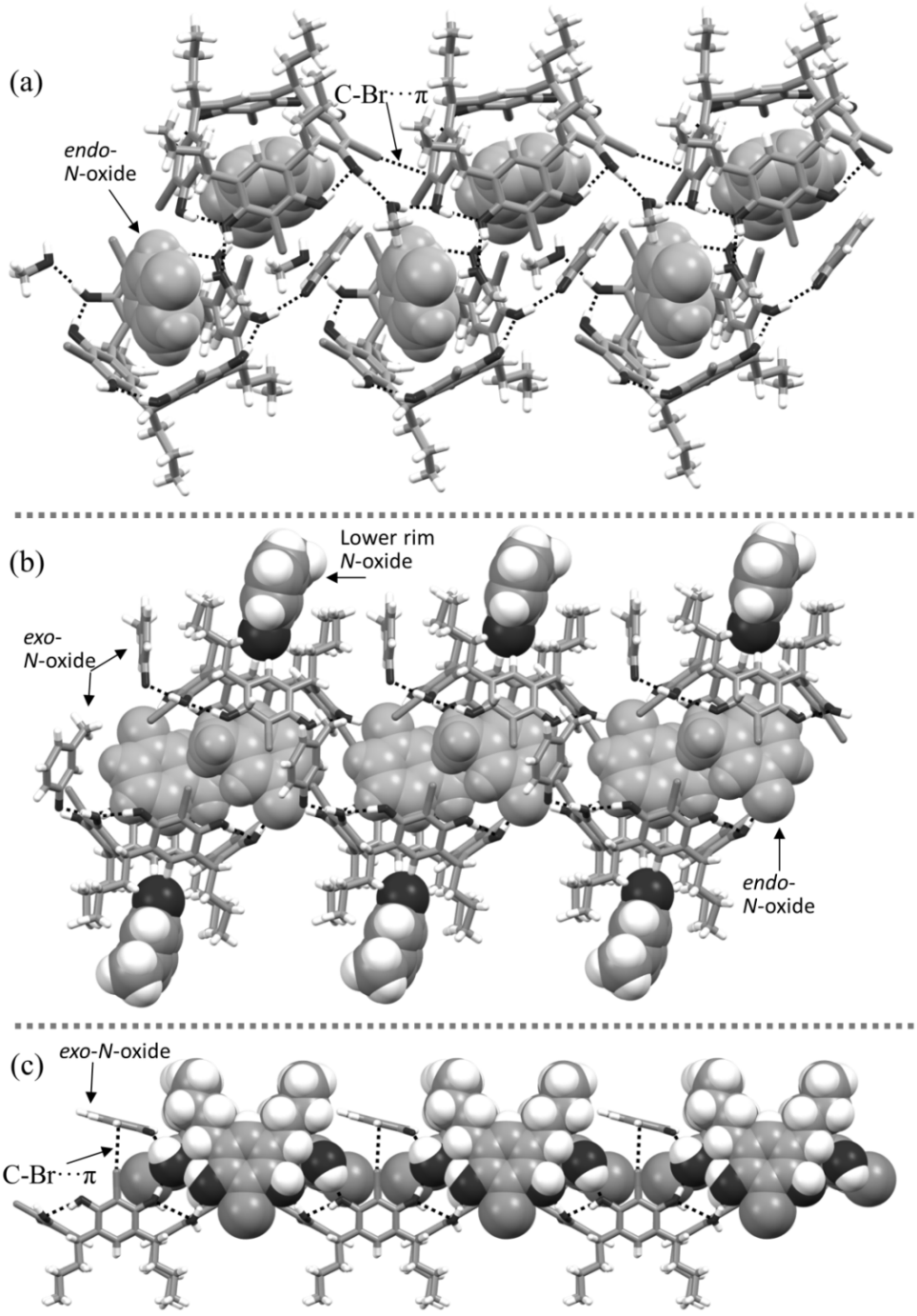

Figure 4. Sections of the 1-D polymeric structures of (a) **1**@**BrC3**_MeOH, (b) **2**@**BrC3**_MeOH (c) **4•BrC3**_MeOH. In (a, b) selected *endo*-*N*-oxide guests are shown as CPK models in pale grey.

The BrC3-*N*-oxide complexes from acetone

In the acetone solutions, the NMR spectra did not show any shielding effects indicating that the *N*-oxide guests are all located outside the host cavity. Crystallization of these same mixtures, through evaporation of the acetone, did however result in providing several *endo*-*N*-oxide complexes. This obvious contrast can be readily explained: at low concentrations, the host-guest interaction is weak, but as the solvent evaporates during crystallization, the increase in concentration combined with favourable packing interactions, results in the formation of favourable *endo*-complexes. All host-guest systems studied crystallized from acetone as *endo*-*N*-oxide complexes: pyridine *N*-oxide (**1**@**BrC3**_acetone), 3-methylpyridine *N*-oxide (**2**@**BrC3**_acetone), quinoline *N*-oxide (**3**@**BrC3**_acetone) and isoquinoline *N*-oxide (**4**@**BrC3**_acetone). The **1**@**BrC3**_acetone crystallized in the monoclinic space group $P2_1/c$. The asymmetric unit contains two crystallographically independent hosts and twelve *N*-oxide guests. Each host accommodates two *endo*-*N*-oxides simultaneously in the cavity. These two 1:2 host:guest complexes form dimeric units with a 2:4 host:guest ratio, and each dimer is held together by *endo*-*N*-oxide N–O···$(H–C)_{guest}$ and N–O···$(H–O)_{host}$ interactions (Figure 5a). The *endo*- and *exo*-*N*-oxides hydrogen bonded to hosts create O···O distances ranging between 2.46 to 2.67 Å. In the 2:4 host:guest dimers, the *endo*-*N*-oxide and host C–Br groups form several weak C–Br···O–N and C–Br···$(C)_{guest}$ interactions with observed short contacts of *ca*. 3.23 Å and 3.50 Å, respectively (Figure 5b). Furthermore, two of the twelve aromatic *N*-oxides are passive towards N–O···$(H–O)_{host}$ interactions, and instead reside in the crystal lattice stabilized through weak N–O···$(H–C)_{guest}$ and N–O···π_{guest} (2.81–2.86 Å) interactions. Overall, the **1**@**BrC3**_acetone has complex 3-D crystal packing and can be

described as **BrC3** hosts embedded in a dense *N*-oxide guest architecture when viewed down the *c*-axis as shown in Figure 5c.

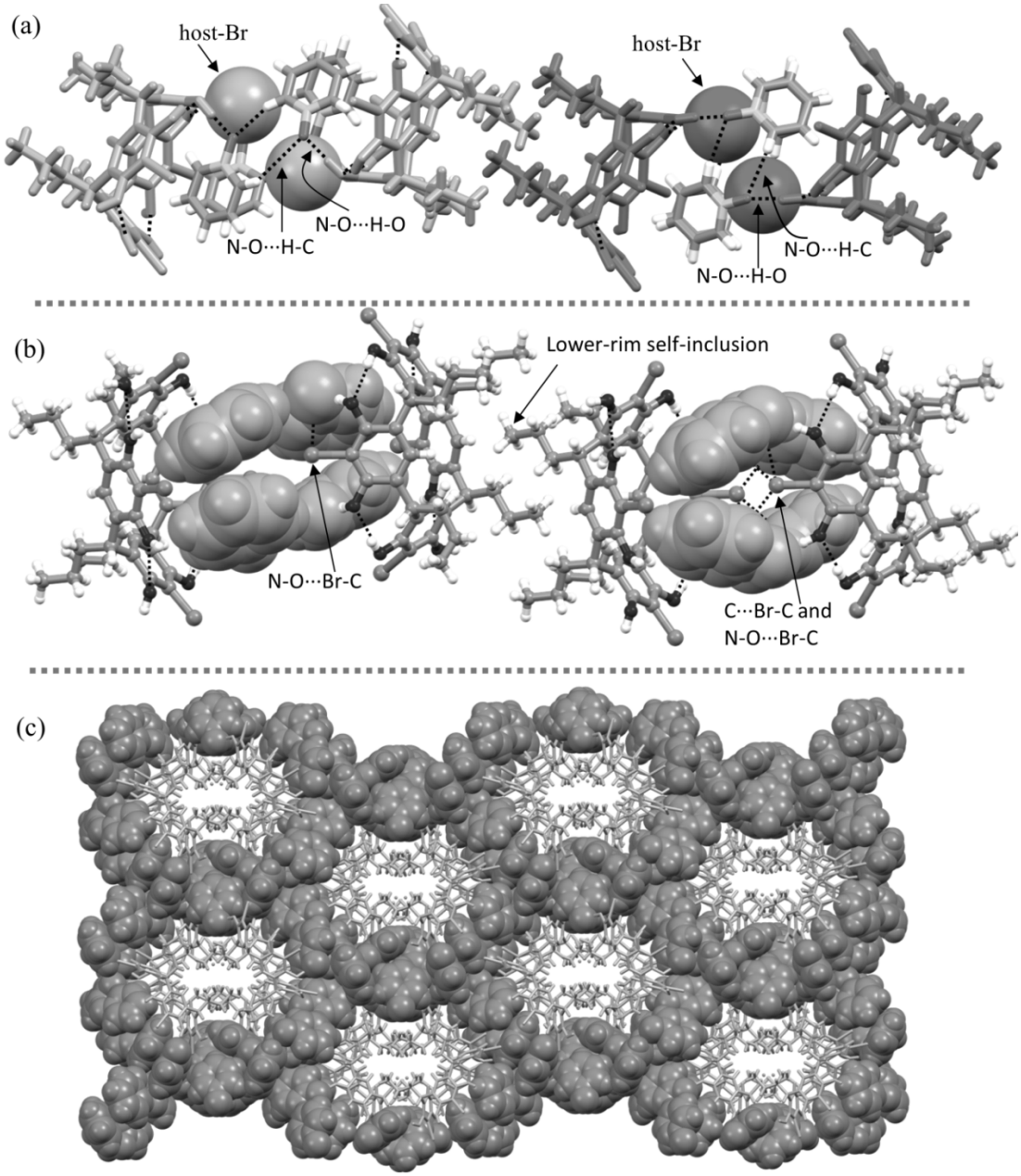

Figure 5. (a) Section of crystal packing showing 2:4 host:guest dimers stabilized through N–O···(H–C)$_{guest}$ and N–O···(H–O)$_{host}$ interactions, and its (b) orthogonal view to show *endo*- C–Br···O–N and C–Br···(C)$_{guest}$ interactions. (c) Cross-section of the 3-D crystal packing viewed down the *c*-axes, hosts (light sticks) embedded in a heavily co-crystallized *N*-oxide guests (dark CPK models).

Complex **2**@**BrC3**_acetone forms a dimeric capsule, {(**2**)$_2$@[**BrC3**]$_2$}•(acetone)$_6$, where the cavity is filled with two *endo*-*N*-oxide guests, as shown in Figure 6a. The aromatic rings of the *N*-oxide guests inside the capsule are separated at centroid-to-centroid distances of 4.86 Å. The dimeric capsule is organized through N–O···(H–O)$_{host}$ and C–H···π (2.66 – 2.96 Å) interactions between the 2:2 (host-guest) molecules in the complex. Although, the carbonyl oxygen of acetone is a potential bidentate HB acceptor, in this case, the acetone molecules are hydrogen-bonded to their hosts *via* C=O···(H–O)$_{host}$ monodentate interactions. This is different from the dimeric (**1**)$_2$@(**MeC2**)$_2$(MeOH)$_2$ host-guest capsule system we have previously reported (*11b*) where the solvent molecules, in that case MeOH, mediated the structure through (O–H)$_{host}$···(MeOH)···(H–O)$_{host}$ interactions forming a tight capsule. In the crystal packing of **2**@**BrC3**_acetone, the capsules extend one dimensionally by *endo*-*N*-oxide $_{host}$(O–H)···N–O···(H–O)$_{host}$ interactions and manifest C–Br···(O-C)$_{host}$ XB contacts at distances of *ca.* 3.0 Å between host C-Br and hydroxyl oxygens as shown in Figure 6b.

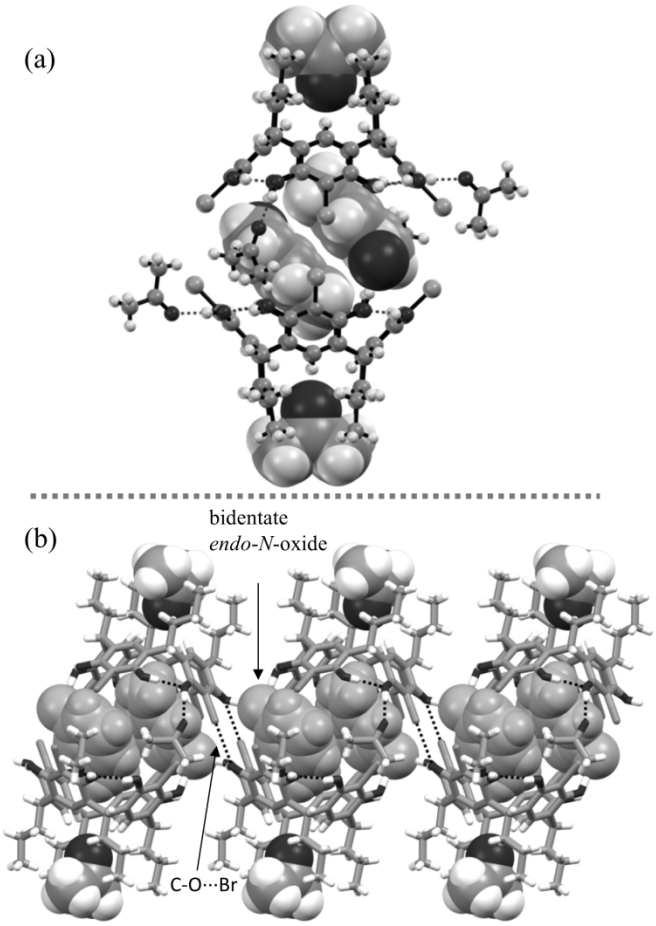

Figure 6. Capsular arrangement of (a) **2**@BrC3_acetone, and corresponding (b) 1-D polymeric structure displaying C–Br···(O-C)$_{host}$ XB contacts. Selected *N*-oxide and acetone molecules are shown as CPK models.

Complex **3**@BrC3_acetone crystallizes in the monoclinic space group *C*2/*c* with a 1:2 host:guest ratio. The *endo*-*N*-oxide guest is extensively stabilized through *endo*-cavity interactions *viz*., C−H···π, C−H···Br and C−Br···C$_{guest}$ (See Figure S5d) and all distances are below the sum of the van der Waals radii. The most notable feature in the 1-D polymeric arrangement is that the (O–H)$_{host}$···N–O···(H–O)$_{host}$ HBs bring the host and guest molecules closer together allowing for the formation of favourable Br···Br (*ca*. 3.55 Å) and C−H···π$_{guest}$ (*ca*. 2.91 Å) interactions (Figure 7a). This close organization was not observed in our previously reported *endo*-complex, **3@BrC2**_acetone (*11f*). The *exo*-*N*-oxides are bidentate HB acceptors bridging the

hosts in a *trans*-fashion through $(O–H)_{host}\cdots(O–N)\cdots(O–H)_{host}$ interactions as shown in Figure 7b. The *trans*-arrangement of *N*-oxide rings over six membered O−H···O HBs may possibly arise due to steric reasons.

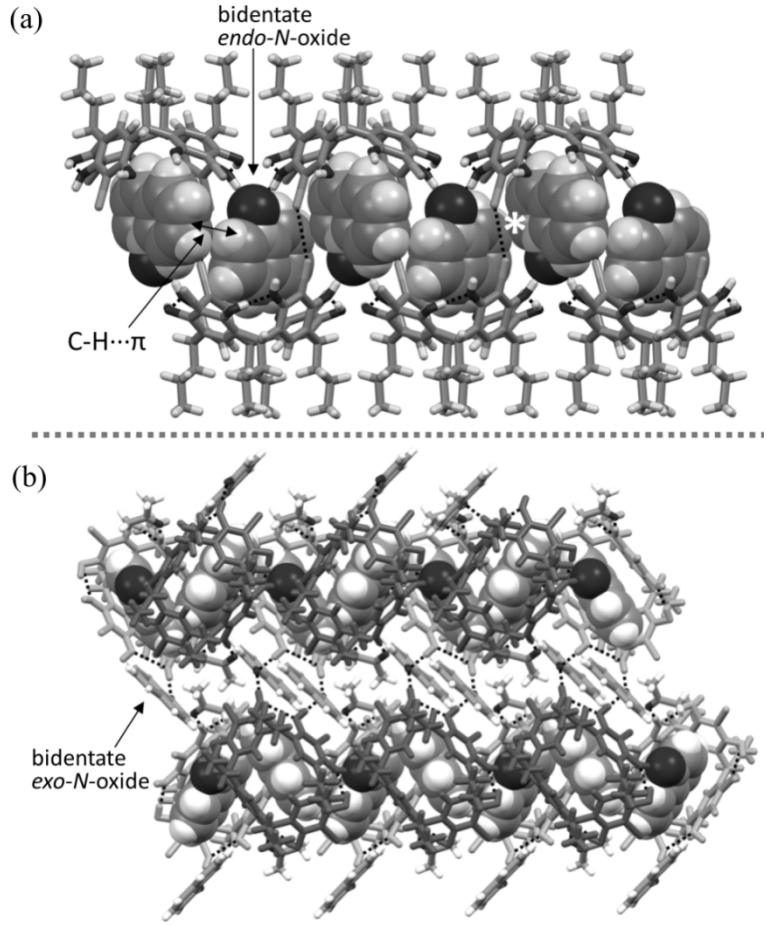

Figure 7. 1-D Polymeric structure to show C−H···π_{guest} ('double headed arrow') and Br···Br (indicated as '*') short contacts driven by e*ndo*-*N*-oxide bidentate N–O···$(H–O)_{host}$ interactions in **3**@**BrC3**_acetone. (b) 2-D Polymeric view for *exo*-*N*-oxide *trans*-arrangement forming cirucular O−H···O HBs.

In all our previous solid-state structures (*11*), when any host (**C1** to **BrC2**, Figure 1) and guest **4** were crystallized from either MeOH or acetone, the guest always resided outside the cavity, hydrogen-bonded to the host hydroxyl group. However, in **4**@**BrC3**_acetone, the *N*-oxide resides inside the cavity stabilized by the C–H···π (*ca*. 2.63 - 2.90 Å) and C–H···Br (*ca*. 2.98 Å) interactions. It also

appears that in contrast to the smaller *N*-oxides, the larger isoquinoline heterocycle prevents capsular formation; instead, it organizes the cavities into a 1-D arrangement similar to **2@BrC3**_acetone with the *endo*-*N*-oxides separated at centroid-to-centroid distances of *ca*. 4.93 Å. In **4@BrC3**_acetone, the N–O···$(H–O)_{host}$ interactions and 1-D arrangement creates N–O···Br XB contacts at distances of *ca*. 3.28 Å, as indicated by the '†' in Figure 8b.

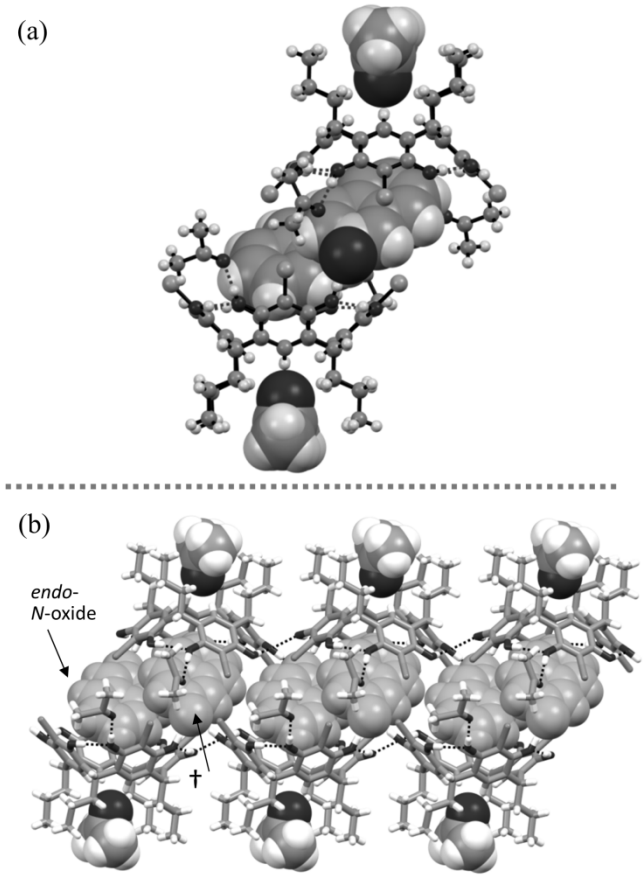

Figure 8. Pseudo-capsular arrangement of (a) **4@BrC3**_acetone, and its (b) 1-D polymeric structure to show e*ndo*-*N*-oxide N–O···Br XB contacts as indicated by '†'. Selected *N*-oxide and acetone molecules are shown as CPK models.

Conclusions

The inclusion behaviour and host-guest properties of C-propyl-2-bromoresorcinarene (**BrC3**) and four aromatic *N*-oxide guests (Pyridine *N*-oxide **1**, 3-methylpyridine *N*-oxide **2**, quinoline *N*-oxide **3**, and isoquinoline *N*-oxide **4**), have been studied in three different hydrogen-bond-competitive solvents, methanol, acetone and DMSO. The study reveals that the molecules interact through different non-covalent interactions in the solution and solid phase, and form *endo*-/*exo*- complexes as characterised by ^{1}H NMR spectroscopy and single crystal X-ray crystallography. In methanol, significant shielding of the ^{1}H NMR signals of aromatic *N*-oxide guests suggests *endo*-complexation similar to that observed in the solid-state structures. In DMSO, no chemical shift changes were observed, which suggests the excellent solvation of both host and guest molecules prevent complexation processes, and this observation is supported by single crystal X-ray structures. In acetone-d_6, contrary to the solid-state analysis, which showed *endo*-constructs, *exo*-aromatic *N*-oxide complexation processes were suggested by the small observed deshielding of the guests' signals. Significant changes in the host -OH resonances suggest these assemblies are driven by hydrogen bond interactions with the upper rim. In the solid-state, the hosts, when crystallized from methanol or acetone, arrange into 1-D self-included chains, while only acetone lattice exhibits Br···Br interactions between adjacent host molecules. The *exo*-complex of **4•BrC3** obtained from methanol, is similar to our previous solid-state structures, while the *endo*-complex of **4** obtained from acetone suggests that the nature of the host-guest assemblies are strongly solvent dependent. The polydentate acceptor nature of *N*-oxides play an important role through N−O···(H−O)$_{host}$ hydrogen bonds by bringing N−O and C−Br groups closer together. This favours C−O···Br and N−O···Br halogen bonds, and C−Br···π_{host} interactions over potential interactions with the solvent. This

study further reinforces the versatility of resorcinarenes as potent receptors and synthons in supramolecular chemistry.

Disclosure statement

No potential conflict of interest.

Acknowledgements

The authors gratefully acknowledge financial support from the Academy of Finland (RP grant no. 298817, KR: grant nos. 265328, 263256 and 292746; RHAR: grant no. 272579), the University of Jyvaskyla, Aalto University, Finland, and the University of Windsor, ON, Canada. This work was supported by the Academy of Finland through its Centres of Excellence Programme (HYBER 2014–2019).

References

(1) (a) Atwood, J. L.; Steed, J. W. *Encyclopedia of Supramolecular Chemistry*; Dekker Encyclopedias Series; M. Dekker, 2004; (b) Sliwa, W.; Kozlowski, C. *Calixarenes and Resorcinarenes*; Wiley, 2009; (c) Pirondini, L.; Dalcanale, E. *Chem. Soc. Rev.* **2007**, *36*, 695–706; (d) Li, N.; Harrison, R. G.; Lamb, J. D. *J. Incl. Phenom. Macrocycl. Chem.* **2014**, *78*, 39–60.

(2) (a) Tulli, L.; Shahgaldian, P. In *Calixarenes and Beyond*; Neri, P.; Sessler, J. L.; Wang, M.-X., Eds.; Springer International Publishing: Cham, 2016; 987–1010; (b) Evan-Salem, T.; Baruch, I.; Avram, L.; Cohen, Y.; Palmer, L. C.; Rebek, J. *Proc. Natl. Acad. Sci.* **2006**, *103*, 12296–12300; (c) Vincent, J.-M. *J. Fluor. Chem.* **2008**, *129* (10), 903–909; (d) Deraedt, C.; Astruc, D. *Coord. Chem. Rev.* **2016**, *324*, 106–122; (e) Faull, J. D.; Gupta, V. K. *Thin Solid Films* **2003**, *440* (1), 129–137.

(3) (a) Spencer, J. N.; Mihalick, J. E.; Paul, I. M.; Nicholson, W. J.; Nicholson, T. J.; Ke, X.; He, Q.; Carter, F. J.; Daniels, S. E.; Fenton, L. J.; Ealy, J. L.; Puppala, S.; Yoder, C. H. *J. Solution Chem.* **1994**, *23*, 711–720; (b) Rekharsky, M.; Inoue, Y. In *Supramolecular Chemistry*; John Wiley & Sons, Ltd, 2012; (c) Schneider, H. J.; Kramer, R.; Simova, S.; Schneider, U. *J. Am. Chem. Soc.* **1988**, *110*, 6442–6448; (d) Nissinen, M.; Wegelius, E.; Falabu, D.; Rissanen, K. *CrystEngComm* **2000**, *2* (28), 151–153; (e) Zhang, Y.; Kim, C. D.; Coppens, P. *Chem. Commun.* **2000**, No. 23, 2299–2300.

(4) (a) Shivanyuk, A.; Rebek, J. *J. Am. Chem. Soc.* **2003**, *125*, 3432–3433; (b) Atwood, J. L.; Barbour, L. J.; Jerga, A. *Proc. Natl. Acad. Sci.* **2002**, *99*, 4837–4841; (c) Evan-Salem, T.; Baruch, I.; Avram, L.; Cohen, Y.; Palmer, L. C.; Rebek, J. *Proc. Natl. Acad. Sci.* **2006**, *103*, 12296–12300.

(5) (a) Mingos, D. M. P.; Braga, D. *Supramolecular Assembly Via Hydrogen Bonds II*; Structure and Bonding; Springer, 2004; (b) Shivanyuk, A.; Saadioui, M.; Broda, F.; Thondorf, I.; Vysotsky, M. O.; Rissanen, K.; Kolehmainen, E.; Böhmer, V. *Chem. – A Eur. J.* **2004**, *10*, 2138–2148.

(6) MacGillivray, L. R.; Atwood, J. L. *Nature* **1997**, *389*, 469–472.

(7) (a) Chapman, R. G.; Sherman, J. C. *Tetrahedron* **1997**, *53*, 15911–15945; (b) Wieser, C.; Dieleman, C. B.; Matt, D. *Coord. Chem. Rev.* **1997**, *165*, 93–161; (c) Scott, M. P.; Sherburn, M. S. Elsevier: Oxford, 2017, 337–374; (d) Deakyne, C. A.; Adams, J. E. Elsevier: Oxford, 2017, 303–342; (e) Mäkinen, M.; Vainiotalo, P.; Rissanen, K. *J. Am. Soc. Mass Spectrom.* **2002**, *13*, 851–861; (f) Shivanyuk, A. *Tetrahedron* **2005**, *61*, 349–352; (g) Baytekin, B.; Baytekin, H. T.; Schalley, C. A. *Org. Biomol. Chem.* **2006**, *4*, 2825–2841; (h) Dalgarno, S. J.; Power, N. P.;

Atwood, J. L. *Coord. Chem. Rev.* **2008**, *252*, 825–841; (i) Ratnaningsih, E. S.; Rahmi, R. *Green Synthesis of Oligomer Calixarenes, Green Chemical Processing and Synthesis*, Iyad, K, **2017** DOI: 10.5772/67804; (j) Shivanyuk, A.; Saadioui, M.; Broda, F.; Thondorf, I.; Vysotsky, M. O.; Rissanen, K.; Kolehmainen, E.; Böhmer, V. *Chem. – A Eur. J.* **2004**, *10*, 2138–2148. (k) L. Turunen, U. Warzok, R. Puttreddy, N. K. Beyeh, C. A. Schalley and K. Rissanen, *Angew. Chem. Int. Ed.* **2016**, 55, 14239–14242. (l) L. Turunen, U. Warzok, C. A. Schalley and K. Rissanen, *Chem.* **2017**, in press.

(8) (a) Ballester, P.; Biros, S. M. In *The Importance of Pi-Interactions in Crystal Engineering*; John Wiley & Sons, Ltd, 2012; pp. 79–107 (*references there in*).; (b) Aragay, G.; Hernández, D.; Verdejo, B.; Escudero-Adán, E. C.; Martínez, M.; Ballester, P. *Molecules* **2015**, *20*, 16672–16686 (*references there in*).

(9) (a) Nissinen, M.; Rissanen, K. *Supramol. Chem.* **2003**, *15*, 581–590; (b) Ma, B.-Q.; Zhang, Y.; Coppens, P. *Cryst. Growth Des.* **2001**, *1*, 271–275; (c) Ma, B.-Q.; Zhang, Y.; Coppens, P. *Cryst. Growth Des.* **2002**, *2*, 7–13; (d) Ma, B.-Q.; Coppens, P. *Cryst. Growth Des.* **2004**, *4*, 1377–1385; (e) Zhang, Y.; Kim, C. D.; Coppens, P. *Chem. Commun.* **2000**, 2299–2300; (f) Zhang, J.; Gembicky, M.; Messerschmidt, M.; Coppens, P. *Chem. Commun.* **2007**, 2399–2401; (g) Ma, B.-Q.; Zhang, Y.; Coppens, P. *J. Org. Chem.* **2003**, *68*, 9467–9472; (h) R. MacGillivray, L.; L. Reid, J.; A. Ripmeester, J. *CrystEngComm* **1999**, *1*, 1–4; (i) MacGillivray, L. R.; Holman, K. T.; Atwood, J. L. *J. Supramol. Chem.* **2001**, *1*, 125–130; (j) Friščić, T.; MacGillivray, L. R. *J. Organomet. Chem.* **2003**, *666*, 43–48; (k) MacGillivray, L. R.; Reid, J. L.; Ripmeester, J. A. *Chem. Commun.* **2001**, 1034–1035; (l) MacGillivray, L. R.; Diamente, P. R.; Reid, J. L.; Ripmeester, J. A. *Chem. Commun.* **2000**, 359–360; (l) Ebbing, M. H. K.; Villa,

M.-J.; Valpuesta, J.-M.; Prados, P.; de Mendoza, J. *Proc. Natl. Acad. Sci. U. S. A.* **2002**, *99* (8), 4962–4966.

(10) (a) Katritzky, A. R.; Lagowski, J. M. *Chemistry of the heterocyclic N-oxides*; Organic chemistry; Academic Press, 1971; (b) Albini, A. *Heterocyclic N-oxides*; Taylor & Francis, 1991.

(11) (a) Puttreddy, R.; Beyeh, N. K.; Rissanen, K. *CrystEngComm* **2016**, *18,* 4971–4976; (b) Beyeh, N. K.; Puttreddy, R.; Rissanen, K. *RSC Adv.* **2015**, *5,* 30222–30226; (c) Beyeh, N. K.; Puttreddy, R. *Dalt. Trans.* **2015**, *44,* 9881–9886; (d) Puttreddy, R.; Beyeh, N. K.; Rissanen, K. *CrystEngComm* **2016**, *18,* 1355–1361; (e) Puttreddy, R.; Beyeh, N. K.; Ras, R. H. A.; Rissanen, K. *ChemistryOpen* **2017**, *6*, 417–423; (f) Puttreddy, R.; Beyeh, N. K.; Ras, R. H. A.; Trant, J. F.; Rissanen, K. *CrystEngComm* **2017**, *19*, 4312–4320.

(12) CSD version 5.38, Update Febraury 2017, Conquest version 1.19

(13) Beyeh, N. K.; Weimann, D. P.; Kaufmann, L.; Schalley, C. A.; Rissanen, K. *Chem. – A Eur. J.* **2012**, *18*, 5552–5557.

(14) (a) Lommerse, P. M.; Stone, A. J.; Taylor, R.; Allen, F. H. *J. Am. Chem. Soc.* **1996**, *118*, 3108–3116; (b) Brammer, L.; Bruton, E. A.; Sherwood, P. *Cryst. Growth Des.* **2001**, *1*, 277–290; (c) Zordan, F.; Brammer, L.; Sherwood, P. *J. Am. Chem. Soc.* **2005**, *127*, 5979–5989.